Article

On the Performance of Proton Exchange Membrane Fuel Cells with a Catalyst Layer Fabricated Using an Inorganic Dispersant with Various Ultrasonic Mixing

Wei-Hsiang Chiang, Shiow-Jyu Lin, and Jong-Shinn Wu*

Read Online

ACCESS | Metrics & More | Article Recommendations

ABSTRACT: This study utilizes both an inorganic dispersant, montmorillonite, and an organic dispersant (AS-1164) with 1.6 and 3.2 mg_{Pt}/cm^2 platinum coatings that underwent various frequencies of ultrasonic mixing (40, 80, and 120 kHz) to fabricate proton exchange membrane fuel cells (PEMFCs). The performance of these PEMFCs was then compared. At room temperature and a hydrogen gas flow rate of 15 sccm. After undergoing 3 h of vibration at 120 kHz, the 1.6 mg_{Pt}/cm^2 platinum-coated organic sample has a power density of 3.69 mW/cm^2, while its inorganic counterpart has an impressive power density of 4.49 mW/cm^2. In addition, using the 1.6 mg_{Pt}/cm^2 platinum-coated inorganic dispersants that underwent vibration at 40 kHz, its resulting power density is only 0.95 mW/cm^2. This result shows that the distribution of platinum coating is more even under high-frequency vibrations than low-frequency ones.
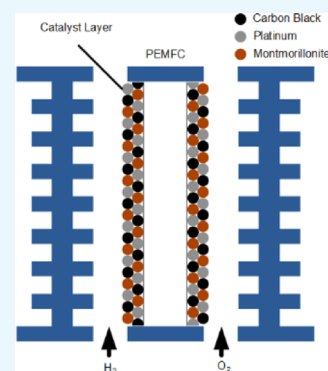
1. INTRODUCTION

In recent years, green energy such as solar and wind energy have been in the spotlight around the globe. However, these forms of energy are considered intermittent energy, as they cannot produce electricity continuously. Consequently, hydrogen gas becomes an ideal method of storing electricity because of its extremely high-energy density.[1] The excess electrical energy produced during peak operation hours can be used to create hydrogen gas and stored, and these gases can then be used for generating electricity when other green methods are not available. Among the various kinds of hydrogen utilization methods, hydrogen fuel cell technology represents one of the most potential energy sources in the near future.[2−4]

There are five main categories of fuel cells:[5−7] proton exchange membrane fuel cells (PEMFCs hereafter), alkaline fuel cells (AFCs),[8,9] solid oxide fuel cells (SOFCs),[10] molten carbonate fuel cells (MCFCs),[11] and phosphoric acid fuel cells (PAFCs).[12,13] AFCs use potassium hydroxide as their electrolyte. If carbon monoxide enters the fuel cell during fuel injection, calcium carbonate may form, blocking ports on the electrodes and decreasing the fuel cell's efficiency. Fossil fuels such as methanol and natural gas are needed to improve the SOFC, MCFC, and PAFC. When compared against other types of fuel cells, the PEMFC possesses advantages, including a short start-up time, low reaction temperature, longevity, and a high-energy density.[14,15]

In general, the PEMFC uses perfluorosulfonate ionomers as electrolytes, platinum or carbon as catalysts, pure or reformed hydrogen gas as the fuel, and air or pure oxygen as the oxidizer.

Its gas diffusion layer is made of carbon fiber paper or carbon fiber cloth that underwent either hydrophobic or hydrophilic treatment, and its carbon or metallic flow field plates also double as bipolar plates.[16] The most critical component in a PEMFC is the proton exchange membrane (PEM)[17] that dictates the lifespan of a PEMFC. The quality of PEMs dictates the lifespan of a PEMFC. A good PEM design must meet the following criteria: a conductivity higher than 0.1 S/m, good chemical stability, good gas sealing capabilities to ensure separation of positively and negatively charged gases, a high level of adhesion to aid the manufacturing of its catalyst layer, and a certain level of structural rigidity.[18] However, to enhance a PEMFC's efficiency, engineers must improve the diffusion layer, catalyst layer, and bipolar plates. One trivial but effective technique to increase the PEMFC's efficiency is to increase the amount of catalyst used.[19] The cost, however, would increase significantly. Thus, other methods such as developing replacement catalyst materials or using multiple catalyst materials are preferred. In addition to new catalyst materials, replacing carbon bipolar plates with metallic plates also improves the fuel cell's efficiency.[20] The downside to using

metallic bipolar plates is that they are more challenging to manufacture. According to previous studies,[21] increasing the reaction temperature is also a viable way to improve efficiency. Treating the anode on a PEMFC with hydrophilic treatments can also enhance its power production performance.[22]

One of the important methods to improve the catalyst layer at a lower cost is to adjust the catalyst's composition. There are many ways to alter catalyst design. The first is to turn platinum into nano-polycrystalline structures and change its form or phase.[23−27] Studies have shown that the smaller the diameter of the polycrystals, the faster the reduction reaction occurs. Another method is to develop catalysts that are not precious metal based.[28−30] Although nonprecious metal catalysts can reduce platinum usage while retaining good reduction capabilities, they lack durability and their cost is still high. Improving the catalyst layer's performance can decrease the adverse effects caused by carbon monoxide,[31−36] decrease platinum usage,[37−41] and increase the rate of hydrogen reduction. For example, Dai et al.[42] have made Pt and W into an alloy that can enhance the electrical catalytic activity of the hydrogen oxidation reaction, which increases the current density up to four times as compared to that of González-Hernández et al.,[43] who used $Pt_2−RuMo/C$ as the catalyst for the PEMFC. Also, the results showed that maximal endurable CO concentration increases with increasing the quantity of Mo(IV). In addition, the stability of the PEMFC increases with an increasing concentration of Ru. Unfortunately, the cost of development and manufacturing is still high. Consequently, other cost-effective methods are strongly needed to decrease platinum usage in catalysts.

In this study, we propose to increase the hydrophilicity of the anode and reduce the usage of platinum effectively by replacing organic dispersants with inorganic montmorillonite and using ultrasonic vibration to disperse carbon black more uniformly. Although we used the same inorganic dispersant as Pai et al.,[44] they manufactured the device under higher pressure and raised the temperature of both the PEMFCs and gases to 50 °C. Instead, we performed the experiments in ambient conditions that utilized only plastic outer casing for the PEMFC, resulting in an easier manufacturing process. The research methods include the preparation of the PEMFC, the experimental methods of observing platinum uniformity and catalyst layer thickness due to various vibration ultrasonic frequencies, and the measurements of the electric properties of the PEMFC is presented next. The corresponding experimental results are presented and discussed. The major findings of the current study are summarized at the end of the paper.

2. RESEARCH METHODS

2.1. Preparation of the PEMFC. The PEMFC catalyst layer is predominantly composed of platinum. To optimize the utilization of platinum, platinum nanoparticles are evenly distributed on the carbon black carrier. This research uses thermal chemical recovery to construct Pt/C-based catalysts by coating platinum onto superconductive carbon black. The performance of this experimental catalyst is then compared against conventional polytetrafluoroethylene (PTFE) heat transfer printed membrane catalysts.

First, carbon black is dispersed with ultrasonic stirring. Its hydrophilicity is improved by using inorganic dispersants. Based on the observation through images taken after the use of inorganic dispersants under various test conditions, for example, Figure 3, the carbon blacks were obviously spread
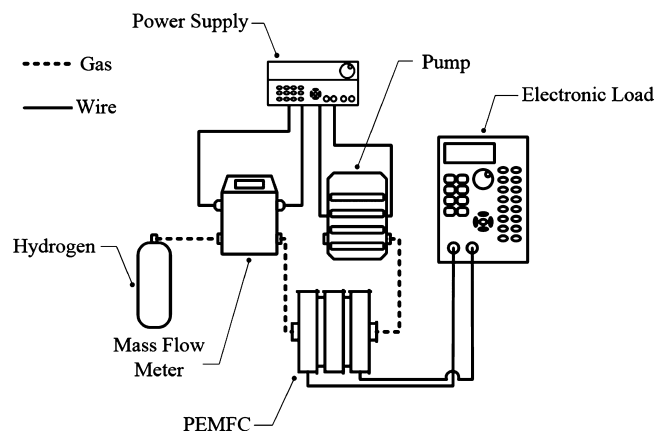
Figure 1. Experimental schematic diagram of PEMFC electrical property measurement.
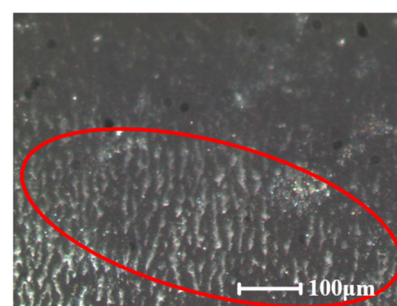
(a) Sample 01
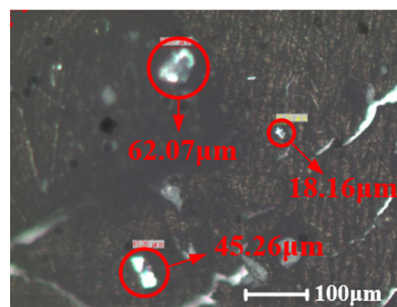
(b) Sample 02
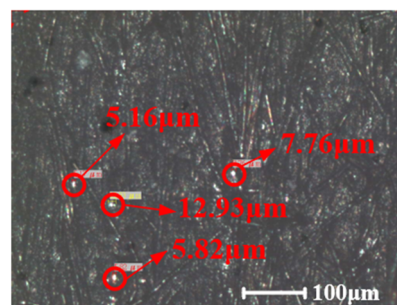
(c) Sample 03

Figure 2. Typical scanning electron microscopy images of catalyst layers under various ultrasonic frequencies. (a) Sample 01 (40 kHz for 180 min); (b) Sample 02 (80 kHz for 180 min); and (c) Sample 03 (120 kHz for 180 min). The abovementioned data are all obtained with clay.
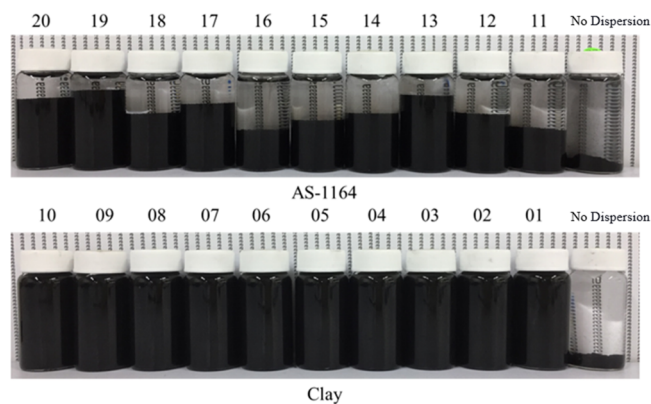
Figure 3. Mixing of carbon black with AS-1164 (top row) and clay (bottom row).

more uniformly with reduced aggregation, which definitely increased the contact surface of carbon blacks with platinum. Then, hexachloroplatinic acid (H_2PtCl_6) extraction of platinum through thermal chemical recovery. The platinum and dispersant are stirred and combined with carbon black under high temperatures to form Pt/C catalysts. The original mass ratio of carbon black to inorganic dispersant is 85:15, with a total mass of 0.1 g. After the mixing of the carbon black with H_2PtCl_6, the Pt/C catalyst was processed so that the total mass was 0.11 g, in which platinum was 0.01 g. Lastly, the Pt/C catalyst is coated on a PTFE film. At a temperature of 125 °C and a pressure of 120 psi, the catalyst is transferred onto both sides of a DuPont Nafion 212 membrane using heat transfer printing. The PTFE films are then stripped off from the Nafion membrane. Multiple Nafion membranes are finally assembled to form a PEMFC. More details of the above-mentioned procedures are described next.

2.1.1. Dispersing Carbon Black Using Montmorillonite and Organic Dispersants under Various Ultrasonic Frequencies. Carbon black is dispersed using ultrasonic stirring. This study investigates the effects of two dispersants: inorganic (montmorillonite) and organic (AS-1164). The weight ratio between carbon black and dispersants is kept at 85:15. Each patch weighs 0.1 g. The solvent chosen is ethanol, as ethanol is more compatible with the choice of materials. The samples are placed into an ultrasonic oscillator. The oscillator has three oscillation frequencies: 40, 80, and 120 kHz. Every sample spends a different amount of time oscillating under the three frequencies.

2.1.2. Coating Platinum on Carbon Black through Thermal Chemical Recovery. This study uses hexachloroplatinic acid (H_2PtCl_6) as the source of platinum. The platinum is coated on carbon black after dispersion through thermal chemical recovery. First, combine the dispersed carbon black with hexachloroplatinic acid, making platinum weight 10% of the total weight. Then, mix ethanol (the solvent) and the mixture mentioned above into the thermal chemical recovery system. Heat the system to 80 °C and stir for an hour, during which the hexachloroplatinic acid decomposes into hydrogen gas, chlorine gas, and platinum. Both hydrogen and chlorine gas are released into the atmosphere after passing through a condenser. Lastly, dry the samples in the open air for 8 h. This concludes the production of the Pt/C catalyst.

2.1.3. Forming Catalyst Layers Using Heat Transfer Printing onto PTFE Films. Add the Pt/C catalysts to 2 mL of the DuPont Nafion solution. Continue stirring until the

sample turns into a paste. Spread the paste onto a 2.5 cm by 2.5 cm PTFE film until the paste has completely adhered to the film. Attach the PTFE films onto both sides of a 3.5 cm by 3.5 cm DuPont Nafion film. Press the layers together at a temperature of 125 °C and a pressure of 120 psi for 180 s. Remove the PTFE films to conclude the manufacturing of the catalyst layer. The presence of the inorganic dispersants in the resulting catalyst layer.

2.2. Characterization Methods. *2.2.1. Measurements of Platinum Distribution and Catalyst Layer Thickness Using an Optical Microscope.* This experiment uses an optical metallurgical microscope (Olympus BX61) capable of 5, 10, 50, and 100 times magnification. Under good lighting and with the aid of a reflecting light source, the magnification is increased slowly, eventually reaching 100 times magnification. To correctly identify the platinum coating, dark-field microscopy is used. Under dark-field microscopy, platinum can be identified by its whitish silver color, while the dark gray color indicates the cracks exposing the carbon carriers. The thickness of the catalyst layer is measured by first slicing a 2.5 cm by 0.1 cm catalyst layer sample, and then placing the said sample onto a metallurgical microscope for measurement.

2.2.2. Measurement of Hydrophilicity Using a Water Contact Angle Machine. The contact angle is defined as the tangent angle between a solid surface and the surface of the fluid. When the contact angle is acute, the cohesion within the fluid is larger than the absorbability between the solid and the liquid. This phenomenon indicates that the solid is hydrophilic. On the other hand, when the contact angle is obtuse, the opposite is true, meaning that the solid is hydrophobic. The contact angle is measured using the machine (Theta Lite optical tensiometers) by dripping water on the sample, observing the interaction between the droplet and the sample using a charge-coupled device camera, and then measuring the angle using built-in protractors in software.

2.2.3. Measurement of PEMFC Electrical Properties. This experiment consists of a mass flow meter, a high-pressure hydrogen gas tank, a power supply, PEMFC samples, a pump, and an electronic load, as shown in Figure 1. First, secure the PEMFC sample onto the electrical load. Attach the gas inlet to the anode of the PEMFC, then attach a mass flow meter to control the flow of hydrogen gas. Connect the cathode to the pump. The supplied voltage shall be set at 1.15 V when taking data, and the hydrogen gas flow rate shall be precisely 15 sccm. Set the electronic load to constant voltage (CV) mode. To measure power generation, slowly decrease the load voltage from 0.9 to 0 V in a 0.1 V increment.

3. RESULTS AND DISCUSSION

3.1. Effect of Vibration Frequency on Platinum Distribution. An increasingly even distribution of platinum increases the probability of contact with hydrogen, which increases the electrochemical surface area (ECSA). In other words, if platinum clumps together, its ECSA is decreased, thus decreasing its reaction rates. Because the clay's surface area with the best test condition is very large, it can adsorb carbon black more uniformly. After the mixing process, both carbon black particles (~30 nm in diameter based on the vendor's data sheet) and platinum particles are adsorbed on the surface of inorganic dispersants. For example, Figure 2c shows the platinum particles in red circles for the Sample 03. Either energy-dispersive X-ray spectroscopy or ECSA measurements should be a much easier approach to directly prove this. We

believe these small clumps are those platinum particles that have been aggregated together. Even though it is relatively subjective, based on the materials and processing procedures we have used for the fabrication of the catalytic layer, we believe the bright spots are platinum. Unfortunately, we were not able to measure the size of the platinum particles due to the limitations of the instrument when the experiments were performed. In addition, it can increase the reaction area of platinum and water, which reduces the platinum clumps and increases the membrane electrode assembly (MEA) efficiency. This experiment aims to study the effects of different vibration frequencies on catalyst layers manufactured using inorganic dispersants using a metallurgical microscope.

As shown in Figure 2, sample one has the worst platinum distribution, with most of the platinum on the surface clumping together in a strip-like pattern. Consequently, Sample 01 (40 kHz, 180 min) has the worst power density of all the inorganic dispersant samples. Sample 03 (120 kHz, 180 min) has the least clumping with an average lump size of 7.92 μm. Sample three shows the least amount of clumping when compared against other samples.

All in all, a higher vibration frequency effectively reduces clumping of platinum on the surface of catalysts. This is apparent when comparing sample two and sample three. Sample 02 was vibrated at 80 kHz for 180 min, showing clear evidence of clumping. Sample 03 was vibrated at 120 kHz for 180 min, with very few traces of clumping.

3.2. Effect of Dispersion Frequency on Hydrophilicity.

The anode of a PEMFC must be hydrophilic to aid in the conduction of protons, increasing its power density because of the hydrated Nafion ionomer. The higher the hydrophilicity, the smaller the contact angle between a water droplet and the surface of the catalyst layer, with the angle approaching zero degrees and vice versa. This study focuses on the testing of samples manufactured using inorganic dispersants. Figure 3 shows a series of images of the mixing of carbon black with AS-1164 (top row) and clay (bottom row). The results clearly show that the mixing of carbon black with clay is much better with a uniform black color compared to the ones with AS-1164. Among these, Sample 13, Sample 19, and Sample 20, with the test conditions referring to Table 1, show much better mixing results with a high-frequency vibration treatment for a longer time. With a shorter dispersion time, Sample 11 and Sample 16 show worse mixing with a clear separation of transparent and black layers. In general, the more the inorganic dispersant was added into the mixture of carbon black and platinum particles, the higher the hydrophilicity.[44] Dispersion of the carbon black and AS-1164/clay improves with an increasing frequency of vibration that leads to higher hydrophilicity. As shown in Figure 4, samples that underwent longer high-frequency vibrations, such as samples 03, 09, and 10, yielded higher hydrophilicity. Their contact angles are 45.50°, 88.88°, and 74.17°, respectively. Samples that underwent shorter periods of high-frequency vibrations, such as Sample 01, yielded a large contact angle (112.43°). These samples are considered hydrophobic. The results, specifically samples 03, 09, and 10, indicate that a high vibration frequency increases the hydrophilicity of the samples. Therefore, the use of the inorganic dispersants with ultrasonic vibration has helped reduce the aggregation of the Pt catalyst. This leads to a higher contact surface area between carbon black and platinum particles that has increased the hydrophilicity as shown in Figure 4.

Table 1. Two Dispersants: Inorganic (Montmorillonite) and Organic (AS-1164) under Various Ultrasonic Frequencies Dispersing Carbon Black[a]

sample	dispersant	ratio (% wt)	40 kHz	80 kHz	120 kHz
01	clay	85:15	180	0	0
02	clay	85:15	0	180	0
03	clay	85:15	0	0	180
04	clay	85:15	60	120	0
05	clay	85:15	60	60	60
06	clay	85:15	60	0	120
07	clay	85:15	120	0	60
08	clay	85:15	120	60	0
09	clay	85:15	0	120	60
10	clay	85:15	0	60	120
11	AS-1164	85:15	180	0	0
12	AS-1164	85:15	0	180	0
13	AS-1164	85:15	0	0	180
14	AS-1164	85:15	60	120	0
15	AS-1164	85:15	60	60	60
16	AS-1164	85:15	60	0	120
17	AS-1164	85:15	120	0	60
18	AS-1164	85:15	120	60	0
19	AS-1164	85:15	0	120	60
20	AS-1164	85:15	0	60	120

[a]Unit: min.
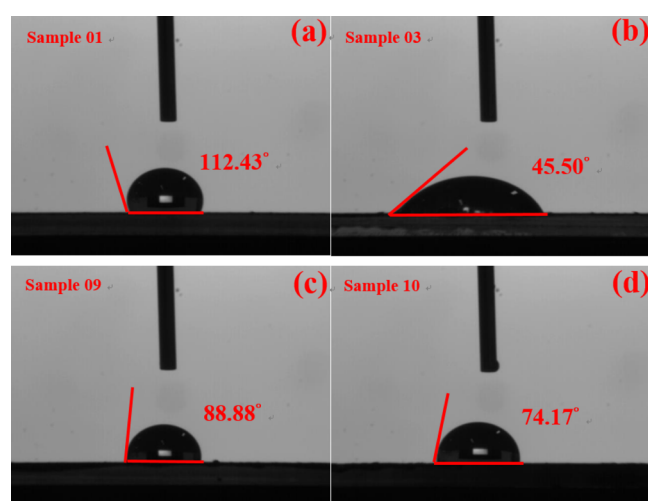
Figure 4. Images of contact angle measurements with different samples. (a) Sample 01 (40 kHz for 180 min); (b) Sample 03 (120 kHz for 180 min); (c) Sample 09 (80 kHz for 120 min and 120 kHz for 60 min); and (d) Sample 10 (80 kHz for 60 min and 120 kHz for 120 min).

3.3. Effect of Vibration Frequency on Electrical Surface Resistance.

Note that the DuPont Nafion 212 membrane used in the PEM has an original thickness of 51 μm and should be reduced when the MEA is mechanically assembled. Using this information, the thickness of the catalyst layer formed using heat transfer printing for 180 s at a temperature of 125 °C and a pressure of 120 psi is between 2 and 2.4 μm. The resistivity can be deduced after measuring the sample's sheet resistance. This is used to study the relationship between the vibration frequency and the catalyst layer's surface resistance. It is well known that lower resistance increases electron conduction, thus increasing its power density. Table 2 shows the derived surface resistivity of samples 01−10. The

Table 2. Surface Resistivity of the Catalyst Layer of Sample 01−10

sample	40 kHz (min)	80 kHz (min)	120 kHz (min)	resistivity ($\Omega\cdot$cm)
01	180	0	0	8.06×10^{-5}
02	0	180	0	6.88×10^{-5}
03	0	0	180	1.04×10^{-5}
04	60	120	0	4.15×10^{-5}
05	60	60	60	3.66×10^{-5}
06	60	0	120	3.25×10^{-5}
07	120	0	60	3.92×10^{-5}
08	120	60	0	4.15×10^{-5}
09	0	120	60	2.35×10^{-5}
10	0	60	120	3.41×10^{-5}

results show that the surface resistance ranges between 1×10^{-5} to 8×10^{-5} $\Omega\cdot$cm, demonstrating that there is no clear correlation between surface resistance and vibration frequency. There is, however, a correlation between surface resistance and material. For example, the measured resistivities of Sample 03 and carbon black only are 1.04×10^{-5} and 8.55×10^{-4} $\Omega\cdot$cm, respectively. From this, the resistivity of Sample 03 with a mixture of carbon black and clay is much lower than that of pure carbon black due to the increased contact surface area caused by the improved mixing of carbon black and platinum particles due to the addition of inorganic dispersants with ultrasonic vibration. Carbon black has a surface resistance of 1×10^{-5} $\Omega\cdot$cm $\pm$ 5% before being dispersed. Therefore, the values measured above are reasonable.

3.4. Effect of Vibration Frequency on the Power Density of PEMFCs. Figure 6 shows the power density of the
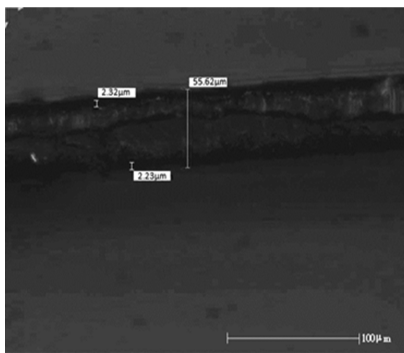
Figure 5. Typical cross-sectional image of the catalysis layer of Sample 03.

PEMFC manufactured using inorganic dispersants under different vibration frequencies. We have plotted the data of power density per unit mass flow rate of hydrogen, unlike most measured data presented in the literature, for a fair comparison of performance. Sample 03 has the highest performance of all the samples, with its peak performance reaching 4.49 mW/cm². On the other hand, samples that underwent fewer high-frequency vibrations, such as Sample 01 purely using 40 kHz for 180 min, performed the worst in power density (0.947 mW/cm²) among all test cases. The test results show that carbon black, with the addition of inorganic dispersants, should have reduced the mass transport regime. However, the kinetic transport regime is extended due to the improved performance caused by the increased contact surface area between carbon black and platinum particles. Samples that underwent longer
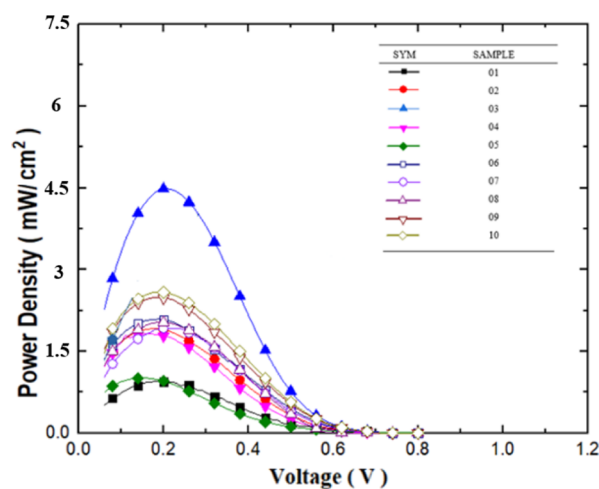
Figure 6. Power density comparison of PEMFCs prepared using inorganic dispersants under different vibration frequencies. Sample test conditions are summarized in Table 1.

high-frequency vibrations generally perform better than samples that underwent low-frequency vibrations.

3.5. Effect of the Dispersant Type on PEMFC Power Density. Figure 7 compares the power density between
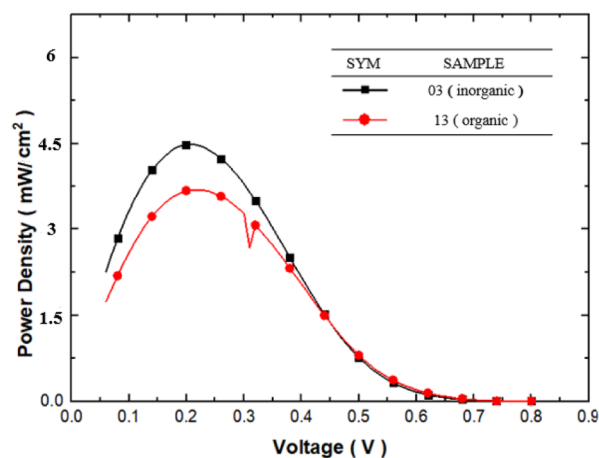
Figure 7. Power density comparison between PEMFCs prepared using inorganic and organic dispersants. Sample 03: inorganic dispersant and Sample 13: organic dispersant.

PEMFCs made using Sample 03 and Sample 13. Note Sample 03 and Sample 13 are the PEMFCs with the catalysis layer fabricated using inorganic and organic dispersants, respectively, per the data presented in Table 1. Both samples have a platinum mass fraction of 1.6 mg$_{Pt}$/cm² without consideration of the ionomer. Sample 03 shows a stable power density curve, while Sample 13's trend is discontinuous at some voltage range. Having a continuous power supply is important for the long-term operation of electronics. Sample 03 has a maximum power density of 0.485 mW/cm², which is 21% higher than that of Sample 13 (3.69 mW/cm²). Under the same ultrasonic vibration condition, PEMFCs manufactured using inorganic dispersants have a higher power density than those using organic dispersants. This is mainly caused by organic dispersant's inability to disperse carbon black, which causes clumping when coating platinum.

3.6. Power Density Comparison PEMFC Samples Prepared Using Inorganic Dispersants. Figure 8 shows
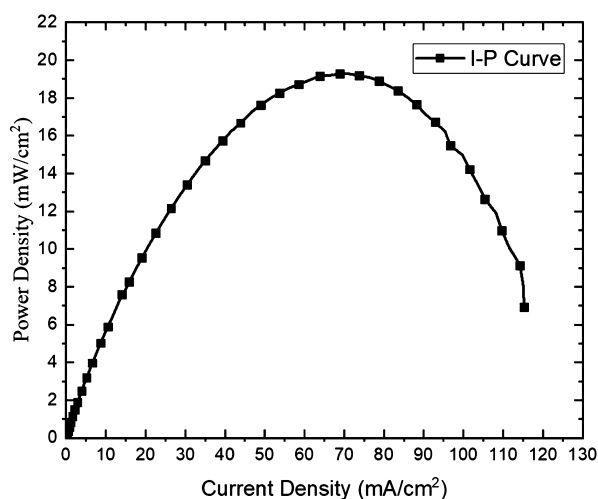
(a)
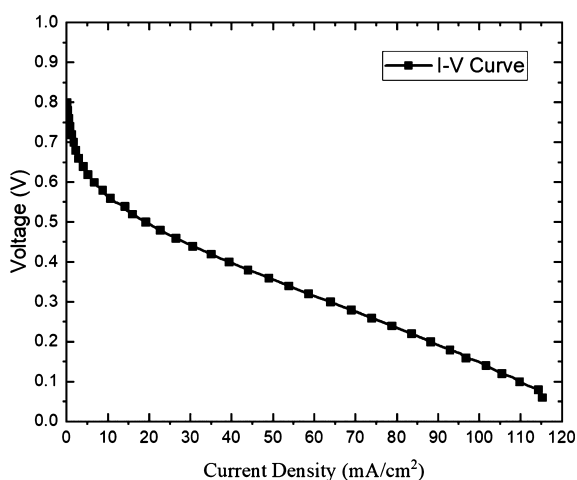
(b)

Figure 8. (a,b) Measured current and power as a function of voltage of modified Sample 03 with 3.2 mg_{Pt}/cm^2 platinum. Sample 03: 120 kHz for 180 min.

the measured current and power of modified Sample 03, designated as Sample 03-1, after raising its platinum content to 3.2 mg_{Pt}/cm^2 for comparison purposes, as a function of the voltage. It has a reaction area of 2.5 cm by 2.5 cm square. The carbon black underwent 180 min of vibration at a vibration frequency of 120 kHz. The ratio between carbon black and dispersant is 85:15 by weight. A commercial GDS210 is used for the gas diffusion layer. At a room temperature of 25 °C, the open-circuit voltage is 0.80 V, and the calculated maximum power density is 19.29 mW/cm^2.

Figure 9 compares the measured power densities of Sample 03, Sample 03-1, and Pai et al.[44] Pai et al.[44] were tested with a reaction area of 5 cm by 5 cm square. Sample 03 and Sample 03-1 both have a reaction area of a 2.5 cm by 2.5 cm square, as described earlier. Sample 03 and Sample 3-1 have platinum mass fractions of 1.6 and 3.2 mg_{Pt}/cm^2, respectively. Their corresponding power densities are 3.3 and 14.4 mW/cm^2, respectively. By doubling the platinum content, the open-circuit current increases almost fourfold. Even though the
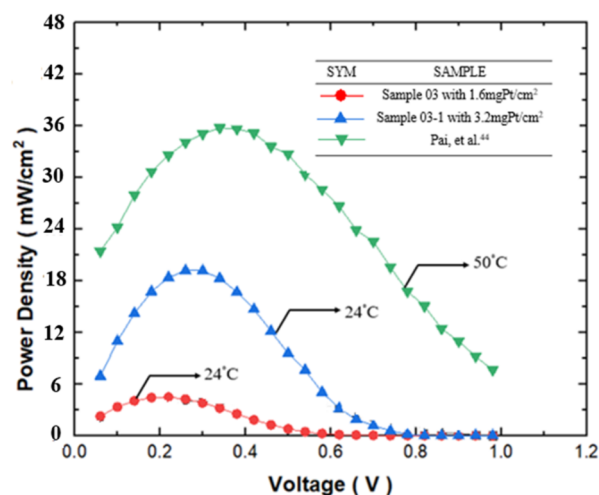
Figure 9. Comparison of power densities of Pai et al.,[44] and PEMFC samples prepared using inorganic dispersants.

performance of Sample 03 is not as good as that presented by Pai et al.[44] with the same inorganic dispersant that was operated at 50 °C, it was operated at ambient temperature (24 °C). That makes the outer casing very easy to make using something like plastics, which further drives the cost down and has high potential in all kinds of applications in daily life.

Sample 03-1 has an open-circuit voltage of 0.80 V, which is higher than the 0.73 V of Sample 03. As shown by Sample 03 and Sample 03-1, not only does the power density increase with the increasing platinum content but there is also an increasing trend in its open-circuit voltage as described in the abovementioned.

For the purpose of clarity of presentation, we have further summarized the measured and previously published data of power densities in Table 3 so it that is easier for future use by the readers.

4. CONCLUSIONS

This study applied an inorganic dispersant (montmorillonite) for dispersing carbon black and platinum with ultrasonic mixing at different frequencies (40−120 kHz) at different times (0, 60, 120, and 180 min) in the catalyst layer and performed comprehensive measurements on the frequency effect on the platinum distribution morphology, hydrophilicity, surface resistivity, and electrical resistance. Moreover, comparisons were made between the electrical performances of the current assembled PEMFCs and Pai et al.[44] The results show that the distribution of platinum particles becomes more uniform with the use of inorganic dispersant under higher ultrasonic vibration frequency for a longer time, in addition to the increased hydrophilicity and reduced surface resistivity of the catalyst layer. The comparison of the power density of the PEMFCs shows that it was 21.51% higher with the use of an inorganic dispersant as compared to that of an organic one. Even though the power density of the current-assembled PEMFCs operating at 24 °C with the proposed fabrication technology is less than that of Pai et al.[44] at 50 °C, it clearly demonstrates the advantage of operating the device at ambient temperature by applying many inexpensive materials. Nevertheless, the current study focuses on the fabrication and operation at an ambient temperature, which might be more cost-effective and widely applicable in the future.

Table 3. Summary of the Measured and Previously Published Data of Power Densities in Figures 5−8

voltage (V)	01	02	03	04	05	06	07 (sample)	08	09	10	13	03-1	Pai[44]
0.1	0.7368	1.66635	3.3243	1.6659	0.94155	1.7976	1.46505	1.67475	2.09595	2.16885	2.59365	10.9707	17.8989
0.2	0.9408	1.8918	4.48065	1.78305	0.9543	2.08065	1.9206	2.031	2.47905	2.583	3.6711	17.6439	29.04945
0.3	0.7416	1.4841	3.7944	1.3377	0.6216	1.6737	1.6704	1.7001	2.0073	2.1465	3.2832	19.1616	34.8699
0.4	0.4032	0.85245	2.16645	0.70215	0.29565	1.03485	1.0029	1.01445	1.22565	1.33245	2.04615	15.74535	35.1447
0.5	0.15195	0.32955	0.76395	0.2496	0.11355	0.44565	0.40395	0.3456	0.53355	0.56955	0.804	9.54405	29.9214
0.6	0.0672	0.07875	0.1632	0.0528	0.0432	0.12	0.1008	0.0096	0.1344	0.144	0.19875	3.97155	22.98195
0.7	0.01125	0.00555	0.0246	0	0.0135	0.0078	0.00225	0	0.0078	0.0135	0.02805	1.1424	15.06915
0.8	0	0	0	0	0	0	0	0	0	0	0	0.0384	8.91105

In summary, the current proposed mixing method between carbon black and platinum using higher ultrasonic vibration frequency for fabricating the catalyst layer is potentially promising in the future due to its potential to possibly lower the manufacturing cost by much less use of platinum, which definitely requires further investigation. Note that the maximum power of a single-cell PEMFC is only 28.035 mW. That is not enough to power a single light-emitting diode. For the demonstration of its practical application in real life, more complex assemblies such as connecting individual cells in series and in parallel are required to increase the power generation. Furthermore, due to the chemical stability of montmorillonite and its inertness toward other compounds, PEMFCs fabricated using montmorillonite may tend to be more stable. With a proper addition amount of the inorganic dispersants, the PEMFC performance will be enhanced. However, the performance will definitely be degraded if added too much.[44] This characteristic is even more prominent when operating at higher temperatures. Therefore, intermediate-temperature PEMFCs[26] fabricated using the current approach definitely deserve further investigation in the near future.

■ AUTHOR INFORMATION

Corresponding Author

Jong-Shinn Wu − *Department of Mechanical Engineering, National Yang Ming Chiao Tung University, Hsinchu 30010, Taiwan*; Phone: +886-3-573-1693; Email: chongsin@faculty.nctu.edu.tw; Fax: +886-3-611-0023

Authors

Wei-Hsiang Chiang − *College of Photonics, National Yang Ming Chiao Tung University, Tainan 71150, Taiwan;* orcid.org/0000-0001-9054-5845

Shiow-Jyu Lin − *College of Photonics, National Yang Ming Chiao Tung University, Tainan 71150, Taiwan*

Complete contact information is available at:
https://pubs.acs.org/10.1021/acsomega.1c05777

Author Contributions

The manuscript was written through the contributions of all the authors. All the authors have approved the final version of the manuscript.

Notes

The authors declare no competing financial interest.

■ ACKNOWLEDGMENTS

■ REFERENCES

(1) Das, V.; Padmanaban, S.; Venkitusamy, K.; Selvamuthukumaran, R.; Blaabjerg, F.; Siano, P. Recent advances and challenges of fuel cell based power system architectures and control - A review. *Renewable Sustainable Energy Rev.* **2017**, *73*, 10−18.

(2) Pollet, B. G.; Staffell, I.; Shang, J. L. Current status of hybrid, battery and fuel cell electric vehicles: From electrochemistry to market prospects. *Electrochim. Acta* **2012**, *84*, 235−249.

(3) Sharaf, O. Z.; Orhan, M. F. An overview of fuel cell technology: Fundamentals and applications. *Renewable Sustainable Energy Rev.* **2014**, *32*, 810−853.

(4) Wilberforce, T.; Alaswad, A.; Palumbo, A.; Dassisti, M.; Olabi, A. G. Advances in stationary and portable fuel cell applications. *Int. J. Hydrogen Energy* **20162016**, *41*, 16509−16522.

(5) *Fuel Cell Technology: Reaching towards Commercialization*; Sammes, N., Ed.; Springer Science & Business Media, 2006.

(6) Blomen, L. J. M. J.; Mugerwa, M. N. *Fuel Cell Systems*; Academic Press: New York, 1993.

(7) Mench, M. M. *Fuel Cell Engines*; John Wiley and Sons Ltd., Academic Press: London, 2008.

(8) Mekhilef, S.; Saidur, R.; Safari, A. Comparative study of different fuel cell technologies. *Renewable Sustainable Energy Rev.* **2012**, *16*, 981−989.

(9) Warshay, M.; Prokopius, P. R. The Fuel Cell in Space: Yesterday, Today and Tomorrow. *Grove Anniversary (1839−1989) Fuel Cell Symposium*, 1989.

(10) Ghorbani, B.; Mehrpooya, M.; Mousavi, S. A. Hybrid molten carbonate fuel cell power plant and multiple-effect desalination system. *J. Cleaner Prod.* **20192019**, *220*, 1039−1051.

(11) Selman, J. R. Research, Development, and Demonstration of Molten Carbonate Fuel Cell Systems. *Fuel Cell Systems*; Academic Press: Boston, MA, 1993; pp 345−463.

(12) Appleby, A. J. Fuel cell technology and innovation. *J. Power Sources* **1992**, *37*, 223−239.

(13) Kordesch, K.; Simader, G. *Fuel Cells and Their Applications*; VCH, 1996.

(14) Devrim, Y.; Albostan, A.; Devrim, H. Experimental investigation of CO tolerance in high temperature PEM fuel cells. *Int. J. Hydrogen Energy* **2018**, *43*, 18672−18681.

(15) Peighambardoust, S. J.; Rowshanzamir, S.; Amjadi, M. Review of the proton exchange membranes for fuel cell applications. *Int. J. Hydrogen Energy* **2010**, *35*, 9349−9384.

(16) Borup, R. L.; Vanderborgh, N. E. Design and testing criteria for bipolar plate materials for PEM fuel cell applications. *MRS Online Proc. Libr.* **1995**, *393*, 151.

(17) Chen, T.; Liu, S.; Zhang, J.; Tang, M. Study on the characteristics of GDL with different PTFE content and its effect on the performance of PEMFC. *Int. J. Heat Mass Transfer* **2019**, *128*, 1168−1174.

(18) Savadogo, O. Emerging membranes for electrochemical systems: (I) solid polymer electrolyte membranes for fuel cell systems. *J. New Mat. Electrochem. Systems* **1998**, *29* (47), no−no.

(19) Sharma, S.; Pollet, B. G. Support materials for PEMFC and DMFC electrocatalysts-A review. *J. Power Sources* **2012**, *208*, 96−119.

(20) Hermann, A.; Chaudhuri, T.; Spagnol, P. Bipolar plates for PEM fuel cells: A review. *Int. J. Hydrogen Energy* **2005**, *30*, 1297−1302.

(21) Rosli, R. E.; Sulong, A. B.; Daud, W. R. W.; Zulkifley, M. A.; Husaini, T.; Rosli, M. I.; Majlan, E. H.; Haque, M. A. A review of high-temperature proton exchange membrane fuel cell (HT-PEMFC) system. *Int. J. Hydrogen Energy* **2017**, *42*, 9293−9314.

(22) Grove Esq, W. R. LXXII. On a gaseous voltaic battery. *London, Edinburgh Dublin Philos. Mag. J. Sci.* **1842**, *21*, 417−420.

(23) Mayrhofer, K. J. J.; Blizanac, B. B.; Arenz, M.; Stamenkovic, V. R.; Ross, P. N.; Markovic, N. M. The impact of geometric and surface electronic properties of Pt-catalysts on the particle size effect in electrocatalysis. *J. Phys. Chem. B* **2005**, *109*, 14433−14440.

(24) Ye, H.; Crooks, J. A.; Crooks, R. M. Effect of particle size on the kinetics of the electrocatalytic oxygen reduction reaction catalyzed by Pt dendrimer-encapsulated nanoparticles. *Langmuir* **2007**, *23*, 11901−11906.

(25) Antoine, O.; Bultel, Y.; Durand, R. Oxygen reduction reaction kinetics and mechanism on platinum nanoparticles inside Nafion. *J. Electroanal. Chem.* **2001**, *499*, 85−94.

(26) Banham, D.; Ye, S.; Pei, K.; Ozaki, J.-i.; Kishimoto, T.; Imashiro, Y. A review of the stability and durability of non-precious metal catalysts for the oxygen reduction reaction in proton exchange membrane fuel cells. *J. Power Sources* **2015**, *285*, 334−348.

(27) Othman, R.; Dicks, A. L.; Zhu, Z. Non precious metal catalysts for the PEM fuel cell cathode. *Int. J. Hydrogen Energy* **2012**, *37*, 357−372.

(28) Dombrovskis, J. K.; Palmqvist, A. E. C. Recent Progress in Synthesis, Characterization and Evaluation of Non-Precious Metal

Catalysts for the Oxygen Reduction Reaction. *Fuel Cells* **2016**, *16*, 4−22.

(29) Higgins, D. C.; Chen, Z. Recent progress in non-precious metal catalysts for PEM fuel cell applications. *Can. J. Chem. Eng.* **2013**, *91*, 1881−1895.

(30) Bashyam, R.; Zelenay, P. A class of non-precious metal composite catalysts for fuel cells. *Nature* **2006**, *443*, 63−66.

(31) Yi, B.; Hongmei, Yu.; Hou, Z.; Lin, Z.; Zhang, J.; Ming, P.; Zhang, H. Electrocatalysts for Proton Exchange Membrane Fuel Cells in Dalian Institute of Chemical Physics, Chinese Academy of Sciences Study on the Pt/C Electrocatalyst. *J. Precious Metal.* **2002**, *23*, 1−7.

(32) Zurowski, A. Cesium and Rubidium Salts of Keggin-Type Heteropolyacids as Stable Meso-Microporous Matrix for Anode Catalyst for H_2/O_2 Proton Exchange Membrane Fuel Cell. *Direct Methanol Fuel Cell and Direct Ethanol Fuel Cell*, Doctoral dissertation, School of Advanced Studies-Doctorate Course in Chemical Sciences (XXI Cycle), 2009.

(33) Garcia, A. C.; Paganin, V. A.; Ticianelli, E. A. CO tolerance of PdPt/C and PdPtRu/C anodes for PEMFC. *Electrochim. Acta* **2008**, *53*, 4309−4315.

(34) Molochas, C.; Tsiakaras, P. Carbon Monoxide Tolerant Pt-Based Electrocatalysts for H2-PEMFC Applications: Current Progress and Challenges. *Catalysts* **2021**, *11*, 1127.

(35) Moore, J. M.; Adcock, P. L.; Lakeman, J. B.; Mepsted, G. O. The effects of battlefield contaminants on PEMFC performance. *J. Power Sources* **2000**, *85*, 254−260.

(36) Jiménez, S.; Soler, J.; Valenzuela, R. X.; Daza, L. Assessment of the performance of a PEMFC in the presence of CO. *J. Power Sources* **2005**, *151*, 69−73.

(37) Secanell, M.; Karan, K.; Suleman, A.; Djilali, N. Optimal design of ultralow-platinum PEMFC anode electrodes. *J. Electrochem. Soc.* **2008**, *155*, B125.

(38) Fofana, D.; Natarajan, S. K.; Hamelin, J.; Benard, P. Low platinum, high limiting current density of the PEMFC (proton exchange membrane fuel cell) based on multilayer cathode catalyst approach. *Energy* **2014**, *64*, 398−403.

(39) Gewirth, A. A.; Thorum, M. S. Electroreduction of dioxygen for fuel-cell applications: materials and challenges. *Inorg. Chem.* **2010**, *49*, 3557−3566.

(40) Gasteiger, H. A.; Kocha, S. S.; Sompalli, B.; Wagner, F. T. Activity benchmarks and requirements for Pt, Pt-alloy, and non-Pt oxygen reduction catalysts for PEMFCs. *Appl. Catal., B* **2005**, *56*, 9−35.

(41) Mayrhofer, K. J. J.; Strmcnik, D.; Blizanac, B. B.; Stamenkovic, V.; Arenz, M.; Markovic, N. M. Measurement of oxygen reduction activities via the rotating disc electrode method: From Pt model surfaces to carbon-supported high surface area catalysts. *Electrochim. Acta* **2008**, *53*, 3181−3188.

(42) Dai, Y.; Liu, Y.; Chen, S. Pt-W bimetallic alloys as CO-tolerant PEMFC anode catalysts. *Electrochim. Acta* **2013**, *89*, 744−748.

(43) González-Hernández, M.; Antolini, E.; Perez, J. Synthesis, characterization and CO tolerance evaluation in PEMFCs of Pt2RuMo electrocatalysts. *Catalysts* **2019**, *9*, 61.

(44) Pai, Y.-H.; Ke, J.-H.; Chou, C.-C.; Lin, J.-J.; Zen, J.-M.; Shieu, F.-S. Clay as a dispersion agent in anode catalyst layer for PEMFC. *J. Power Sources* **2006**, *163*, 398−402.